

# Distorted Path Analysis of Different Layered Soil Pressurized Under Uniform Displacement Rate: A Laboratory-based Study

MD. Nazmul Islam Rafi<sup>1</sup>, Mohammad Shahidur Rahman<sup>2</sup>, Fatema Tarin<sup>3</sup>, Mahmoud Ibne Sadeque<sup>4</sup>

<sup>1</sup>Lecturer, Dept. of Civil Engineering, Leading University, Sylhet-3112, Bangladesh,

<sup>2</sup>Professor, Dept. of Civil and Environmental Engineering, Shahjalal University of Science and Technology, Sylhet-3114, Bangladesh,

<sup>3</sup>Graduate, Dept. of Civil and Environmental Engineering, Shahjalal University of Science and Technology, Sylhet-3114, Bangladesh

<sup>4</sup>Graduates, Dept. of Civil and Environmental Engineering, Shahjalal University of Science and Technology, Sylhet-3114, Bangladesh

\*\*\*

**Abstract** - Geotechnical modeling requires precise measurement of soil deformation to be effective. Understanding the final collapse process of a geotechnical structure depends on measuring gross deformations. A geotechnical model's post-test excavation often allows for the observation of gross or ultimate displacements. These measures serve as a "before" and "after" snapshot of the model, enabling estimation and calculation of the failure mode. Currently, a grid of target markers placed in a plain of exposed soil is tracked via a series of video shots. The analysis of distorted paths for various soil forms using a cheap, adaptable technology is described in this study. It allows for non-contact assessment of soil deformation at pre-failure strain levels without the need for target markers. This system combines digital photography and image analysis. It finally will lead to getting a better understanding of competent soil formation which is required to meet the ever-growing need for rehabilitation and expansion of civil infrastructures. From the study, it can be summed up, which formation of soil is better for foundation design and decisions can be made about different soil improvement techniques for different soils and soil formations. This study helps to conclude with different numeric data that all sandy soil formation is the best for foundations as the deformation width is higher, resulting in less settlement whereas all clayey formation is the worst case.

World Bank) and the infrastructure investment has reached \$6 billion in 2016-17 from \$2 billion in 2011-12 (The Daily Star 2017). To fulfill the constantly expanding requirements of society, civil infrastructure must be renovated and expanded. However, the capacity to do so is directly impacted by the availability of suitable soils. The assessment of large deformations is often essential to comprehending the eventual process of collapse of a geotechnical structure [1]. Serviceability state design necessitates an understanding of settlements and ground developments at significantly lower stresses in contrast to the substantial deformations found in the extreme state [1]. Compressive and elastic stresses, which often appear when soil shears, are the cause of the deformation observed in the soil [2]. Because soil sensors can't provide a continuous view of the intentional continuum, model studies to measure three-dimensional deformation patterns inside a soil mass are constrained. Additionally, soil sensors exhibit static and dynamic properties that are distinct from those of the surrounding soils, changing how the deliberate continuum responds [3].

Imaging technologies are progressively being utilized to consider numerous geotechnical issues. For instance, a framework was created to consider the conveyance of voids in soil examples [4]. A Vision Cone has likewise been created for in-situ soil investigation, and procedures were created to utilize its caught pictures in soil portrayal [5].

For analyzing the distorted path, many organizations and scientists have tried to develop tools and methods. Among these, one of the most reliable techniques is the "Digital Image Correlation (DIC)" process. "Digital image correlation (DIC)" is a distortion estimation method in progressively boundless use over a wide scope of experimental mechanics research disciplines [6], [7]. In recent years, the geotechnical engineering community has adopted digital image correlation methodologies,

**Key Words:** Imaging Technology, Distorted Path, Deformation, Image Analysis, Digital Photography, Soil Formation.

## 1. INTRODUCTION

Population and civil infrastructure continue to expand at an unprecedented rate. The population of Bangladesh (about 163 million) is growing at an annual rate of 1.1% (2016) (Population and growth rate of Bangladesh 2016-

providing professionals with a revolutionary tool for the visualization of failure processes and the evaluation of soil and soil-structure interaction behavior in physical model experiments [8]. But a few things can alter how precise and accurate DIC is. Some of them are subset surface and size, camera commotion, the decision of subpixel addition conspires, and the camera geometry mistakes related to without-of-plane development, self-warming, and the complexities of mentioning objective facts through thick transparent windows [8].

The first measurements of displacements inside a soil mass were made by Gerber (1929) using an X-ray approach in which led bullets are implanted in the soil model. Progressive radiographs are acquired to follow the passage of these markers in huge sand models and shear devices to determine incremental strain patterns. [9]. Through the use of large (2.0 m x 0.5 m) models, with an accuracy of 0.1 percent, the technology was successfully employed to produce volumetric strain and shear contours.[10].

Beginning in the late 1990s, researchers wound up mindful that DIC was likewise especially appropriate to geotechnical engineering applications [1], [3], [11]– [14]. Although the most well-known use of DIC in geotechnical engineering is geotechnical centrifuge modeling, which prohibits the exposure of radiographs in flight, choosing the right image texture for measurements in soils was one of the first tasks when applying DIC methods in geotechnical engineering measurement applications [1], [11]. Modelers changed the approach instead by including a transparent window that shows the model's plane where the target markers are positioned. However, this transparent sidewall is required to have enough stiffness to simulate plane strain conditions under loading, leading to typical acrylic window thicknesses of up to 76 mm. This large window causes extra refraction-related mistakes as well as changes the optics of errors brought on by out-of-plane deformation and camera self-warming. Additionally, the camera pieces will rotate and deflect concerning the measurement plane within the transparent window if the physical model test is carried out using the centrifuge modeling technique under enhanced gravity. This large window causes extra refraction-related mistakes as well as changes the optics of errors brought on by out-of-plane deformation and self-warming of the camera. Additionally, the camera pieces will rotate and deflect concerning the measurement plane within the transparent window if the physical model test is carried out using the centrifuge modeling technique under enhanced gravity. It goes on to explain that if the camera lens is viewed as a cantilever beam, growing self-weight causes the lens body to deflect downwards whereas the scene in the image seems to move higher [12]. In-flight strain measurements are presented by Beasley (1973) and Mair (1979) to a

resolution of 1 percent, from a measurement accuracy of 100  $\mu\text{m}$ . [15], [16].

Video capture has lately been used to monitor deformations in centrifuge tests [17], and attempts have been made to assess triaxial test deformation using video footage [18]. The use of video photography can eliminate the requirement for the time-consuming calculation of exposed film. The image processing technique of centroiding may be used to evaluate the area of a large number of target markers. Centroiding is accounted for in the states of a common geotechnical model for identifying target markers to an accuracy of 0.1 pixels [19]. Taylor et al. (1998) provide a centroiding-based estimate approach capable of tracking the movement of 3 mm diameter target markers implanted in clay with an accuracy of 60-105  $\mu\text{m}$  over a 300 x 200 mm field of view [20]. Grant (1998) introduces an example of following displacement measurements as strain contours with a resolution of 1% [20], [21].

Particle Image Velocimetry is an alternate method for assessing soil deformation using a sequence of digitally acquired photographs (PIV). Particle Image Velocimetry (PIV) is a velocity-measurement technology that tracks texture patches through an image sequence [1]. This advanced velocity monitoring approach originated in fluid mechanics, where the flow field of a fluid may be investigated by seeding the flow with marker particles and following the movement of tiny patches within a broader picture [22]. Soil deformation can be thought of as a low-velocity flow phenomenon. In fluid mechanics testing, polystyrene balls or colored powder are introduced to the flow field to provide an identifiable texture for image processing. Natural sand, on the other hand, has its texture in the shape of varied colored grains, as well as the light and shadow framed between continuous grains when illuminating a plane of granular material. Texture can be imparted to an exposed plane of clay by using colored 'flock' or fine sand.

The Particle Image Velocimetry (PIV) approach is similarly relevant to triaxial testing and has been demonstrated to have adequate resolution to quantify pre-failure stresses as well as the flexibility to record non-homogeneous deformations that are unseen to traditional transducers [11].

That's why in this study, imaging technology was chosen for demonstrating the distorted path of different layered soil when the load was applied to the soil deposition. A high-resolution camera was utilized to capture pictures of the soil deposition before and then afterward the distortion. Next video editing process was performed to take snapshots at 5 seconds intervals of up to 30 seconds for analyzing the distorted path of different layered soil. A model has been developed to measure deformations

inside different soil depositions. In this situation, an underlying reference picture is utilized to catch the visual appearance of the example surface before loading. Six pictures are then taken to catch the visual appearance of the distorted layers under load. The finding of the study should be applied to serving people to let them know about the settlement condition and distorted path of soil on which the superstructure will be constructed. The experiment was performed in "The Geotechnical Engineering Laboratory" at Shahjalal University of Science and Technology, Sylhet, at the Department of Civil and Environmental Engineering. The soils were collected from the clay modelers. The tests were performed in a non-water table and dry condition. The objective of this study was to design and fabricate a comprehensive experimental protocol to measure the settlement of soil deposition in different conditions by analyzing the distorted path of different layered soil.

## 2. METHODOLOGY

There were four main components of the proposed study such as i) design of the product ii) fabrication of the product and finally iii) Validation and iv) Application of the product. The flow diagram of the general framework of the research activities is shown in Chart -1.

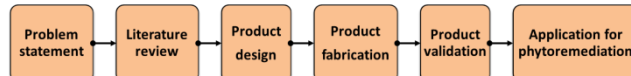


**Chart -1:** General framework of the research works

### 2.1 Design of the Experimental Model

A transparent chamber was made using steel around its corner so that the chamber stays strong. The load was applied to the model along with the sample to check its validation and finally, after several trials, the required model was designed to conduct different test experiments. As illustrated in Chart- 2 the flow diagram shows the design approach for the fabrication of the model.

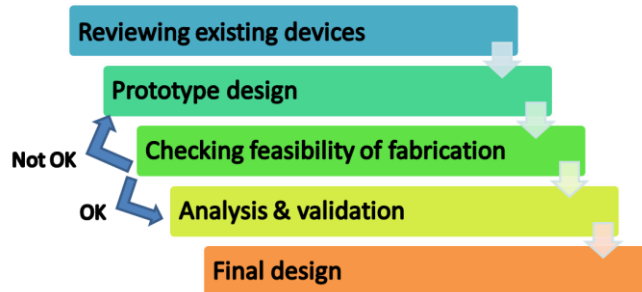


**Chart- 2:** A design approach for the fabrication of the experimental model

Some factory-made materials and tools were also used to maintain the serviceability and precision of the

experimental model. The model is comprised of four transparent sides which has hold tight using an iron frame. Then a thick iron plate was used as a footing by which the total load applied was imposed to the sample formation. A front view of the chamber is shown in Fig- 1.

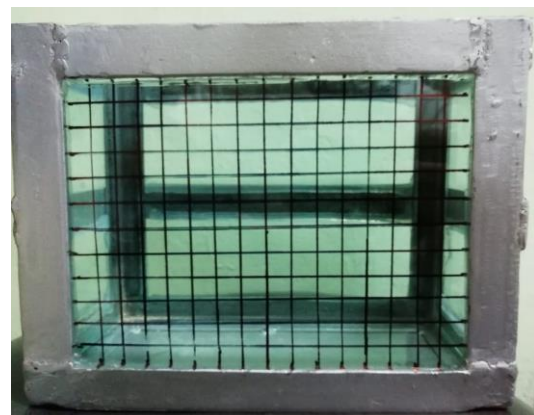


**Fig-1:** Front view of the Model

### 2.2 Fabrication of the model

This part presents the product details of the experimental model for the tests. All the elements are enunciated of technical specifications, instrumental details, diagrams, images, and testing procedures. The device was planned to fabricate cost-effectively. Locally available commercial materials along with some commercial parts were used to build the setup. The model apparatus has some internal and external supporting gadgets. The glasses were first made airtight using silica gel, then it was connected to the external frame to give them a firmer structure. The frame steel was 1 inch in thickness and fully polished and painted. On the other hand, a footing was made using a thick iron. The thickness of around 10mm. The frame's dimensions as first calculated are 10 inches in length, 8 inches in height, and width to be 4 inches in. The glass thickness was 10 mm high-quality glass. The glasses are attached at the inside of the frame making a clear space of 9-inch length and 3.5-inch width. Thus, the footing is made of a width of 3.5 inches and 2 inches in length, so that it can help in bulging the soil when the load was applied.

The whole apparatus was designed keeping in mind the real-world scenario and real-world soil stratification and formation. The load was applied similarly too

### 2.3 Description of the 'Experimental Setup'

#### 2.3.1 Experimental Model

The 10 mm glasses on the four sides make easily visible the deformation when the load is applied. The glasses were made airtight using silica gel and then connected to the inside of a steel frame which was made of thick 1-inch

steel. These steels were welded together and formed a structure of containers. The glass container was put inside of it.

Once the model was set up, it was time for the soil layers to be put in and applied load. The pulverized clay was collected from sand modelers. Those were some packs of clays. Those were ground first then oven-dried to get the required pulverized clay. And the other sand was the sand of the Shari River which is normally used for the filling-up process. It was sieved and oven dried and then put into the experiment.

### 2.3.2 Properties of Dry Sand

After calculation, the properties of dry sands for the research were found.

- Dry Unit Weight =  $26.095 \text{ kg/m}^3$
- Specific Gravity = 2.66
- From the grain size distribution curve, it can be said that the particle size distribution of sand is well-graded.
- The density of 1 layer of sand to be put in the experimental setup =  $0.024 \text{ kg/m}^3$

### 2.3.3 Properties of Pulverized Clay

After calculation, the properties of pulverized clay for the research were found.

- Dry Unit Weight =  $26.487 \text{ kg/m}^3$
- Specific Gravity = 2.70
- Plastic Limit, PL= 22.7%
- Liquid Limit, LL= 56.26%
- Plasticity Index PI= 33.56%
- Density of 1 layer clay is =  $0.016 \text{ kg/m}^3$

### 2.3.4 Camera and Tripod

A high-resolution mobile camera was used to video shoot the loading and with a tripod to remove the shakiness of the video. Later video analysis was done on adobe premiere pro software and finally, analysis was done on the still images which were captured from the video.

## 3. RESULT AND DISCUSSION

### 3.1 Distortion Behavior of Soil

To observe the distortional behavior closely, the soil was put into the experiment with different formations, keeping the real-world scenario in mind. In the Fig-2, the red demarcation line denotes the deformation at the joint of the layers. The blue line denotes the general shear failure path, and the green line denotes the direction of the

punching shear. All the testing cases are shown from Fig-3 to Fig-8.

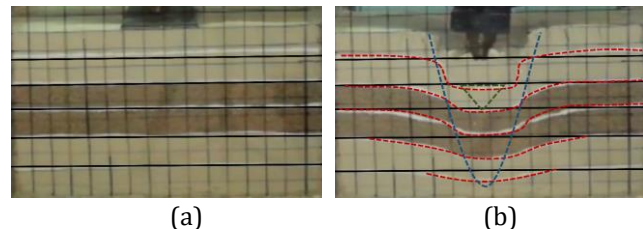


**Fig-2:** Soil before and after failure.

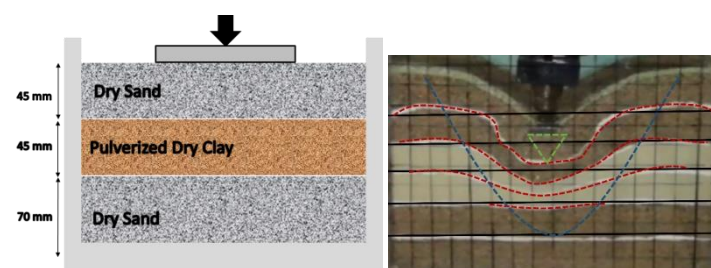


**Fig-3:** Case 1 Soil formation and failure.

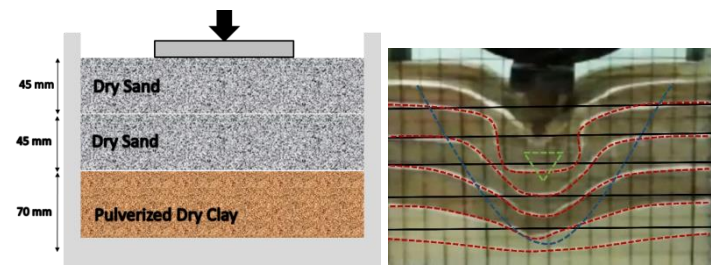


**Fig-4:** Case 2 Soil formation and failure.

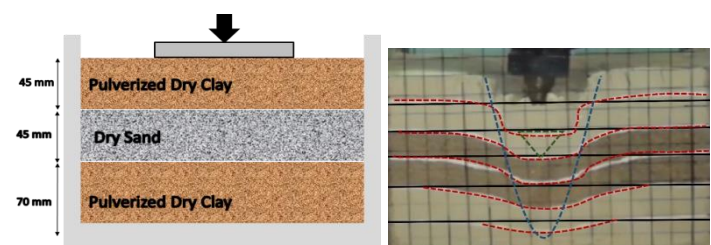


**Fig-5:** Case 3 Soil formation and failure.

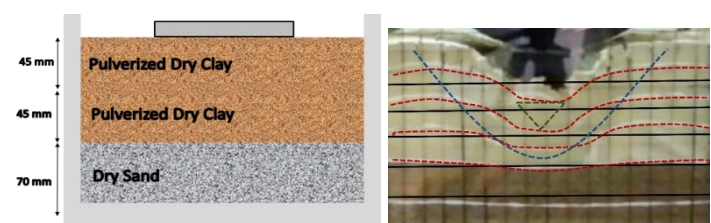


**Fig-6:** Case 4 Soil formation and failure.

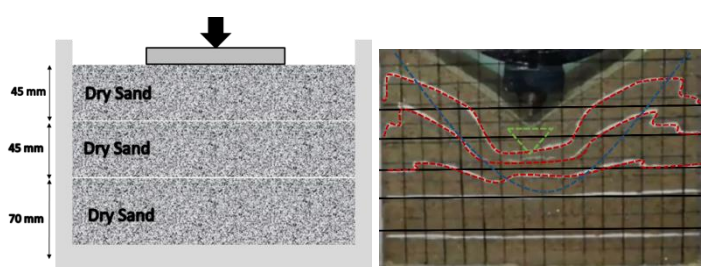


**Fig-7:** Case 5 Soil formation and failure.

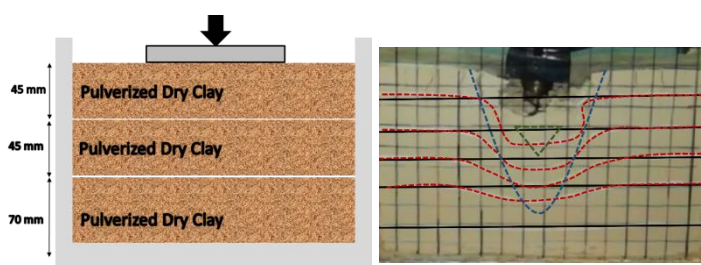


**Fig-8:** Case 6 Soil formation and failure.

### 3.2 Observed Deformations

The figures show the deformation behavior from snapshots taken during each test at 5, 10-, 15-, 20-, and 25-seconds displacement, and the deformation behavior in each instance was precisely observed during each test. The maximum vertical height of the heave, the offset of this maximum height from the edge, and the width of the deformation were noted during the experiment.

Between the models, a clear piece of glass with a printed grid was used to help scale the geometry of the deformation behavior, with each square on the grid measuring 0.5 inches by 0.5 inches, and the deformation values are shown in Tabl-1.

From the calculations, while summing up it can be said based on the width of the deformation zone because the more the width of the deformation, the less the settlement makes the distribution of load to a greater area.

Case 5 gives the most definitive result and shows deformations in such a way that it proves that it is the most suitable in the real-world scenario. As the width of the deformation is the highest inch is about 8 inches.

And cases 4 and 6 give the worst result as the width of the deformation zone is the lowest and resulting in more settlement in a definite area.

So, the whole clayey layer is not at all suitable for foundations whereas the whole sandy layer is the best fitted and perfect zone for the foundation.

Table 4.1: Observed Deformations

			Cases					
			1	2	3	4	5	6
15 Sec	Maximum height (Inch)	heave	0.5	0.5	0.25	0.25	0.5	0.25
	The offset of maximum heave height (inch)	2	2	1	1	2.5	1.5	
	Overall width of deformation zone (inch)	5	4	3.5	3	7.5	2	
25 Sec	Maximum height (Inch)	heave	1	1	0.5	0.5	1	0.5
	The offset of maximum heave height (inch)	2.5	2.5	1.5	1.5	3	3	
	Overall width of deformation zone (inch)	6	5	3.5	3	8	3	

## 4. CONCLUSION

### 4.1 Statement of findings

Important findings of the study could be listed below-

- This study proposed a unique idea to design a cost-effective experimental setup in the laboratory using locally available materials.
- It also described a simple procedure to find out the competent soil formation by checking the distorted path after the load is applied using imaging technologies.
- The developed tool can give an assumption of the real-world scenario and the settlement of the soil.
- The tool can finally be used as a powerful tool for studying deformation inside soils non-intrusively.

### 4.2 Final Output of the Study

While summing it can be said based on the width of the deformation zone because the more the width of the

deformation, the less the settlement makes the distribution of load to a greater area.

The whole sandy soil layers give the most definitive result and show deformations in such a way that it proves that it is the most suitable in the real-world scenario. As the width of the deformation is the highest inch is about 8 inches.

And the whole clayey layers give the worst result as the width of the deformation zone is the lowest and resulting in more settlement in a definite area.

So the whole clayey layer is not at all suitable for foundations whereas the whole sandy layer is the best fitted and perfect zone for a foundation.

## REFERENCES

- [1] D. J. White, M. D. Bolton, D. J. White, W. A. Take, and M. D. Bolton, "Measuring soil deformation in geotechnical models using digital images and PIV analysis SEE PROFILE Measuring soil deformation in geotechnical models using digital images and PIV analysis," pp. 997–1002, 2001, Accessed: Aug. 31, 2022. [Online]. Available: <https://www.researchgate.net/publication/237262677>
- [2] R. Jewell, "Soil reinforcement with geotextiles," 1996, Accessed: Aug. 31, 2022. [Online]. Available: <https://agris.fao.org/agris-search/search.do?recordID=US201300016528>
- [3] S. Sadek, M. Iskander, J. L.-J. of computing in civil, and undefined 2003, "Accuracy of digital image correlation for measuring deformations in transparent media," *researchgate.net*, 2003, doi: 10.1061/(ASCE)0887-3801(2003)17:2(88).
- [4] J. Frost, C. K.-G. T. Journal, and undefined 1996, "Automated determination of the distribution of local void ratio from digital images," *astm.org*, Accessed: Aug. 31, 2022. [Online]. Available: [https://www.astm.org/DIGITAL\\_LIBRARY/JOURNALALS/GEOTECH/PAGES/GTJ10334J.htm](https://www.astm.org/DIGITAL_LIBRARY/JOURNALALS/GEOTECH/PAGES/GTJ10334J.htm)
- [5] S. A. Raschke and R. D. Hryciw, "Vision Cone Penetrometer for Direct Subsurface Soil Observation," *Journal of Geotechnical and Geoenvironmental Engineering*, vol. 123, no. 11, pp. 1074–1076, Nov. 1997, doi: 10.1061/(ASCE)1090-0241(1997)123:11(1074).
- [6] B. Pan, K. Qian, H. Xie, and A. Asundi, "Two-dimensional digital image correlation for in-plane displacement and strain measurement: A review," *Meas Sci Technol*, vol. 20, no. 6, 2009, doi: 10.1088/0957-0233/20/6/062001.
- [7] M. Sutton, J. Orteu, and H. Schreier, *Image correlation for shape, motion and deformation measurements: basic concepts, theory and applications*. 2009. Accessed: Aug. 31, 2022. [Online]. Available: <https://books.google.com/books?hl=en&lr=&id=AkqMxpQMLsC&oi=fnd&pg=PA1&dq=Image+correlation+for+shape,+motion+and+deformation+measurements.+&ots=5WjU9aDD3H&sig=vH-urSKgnNUxM9eAoMLmODy0wpo>
- [8] W. A. Take, "Thirty-sixth canadian geotechnical colloquium: Advances in visualization of geotechnical processes through digital image correlation," *Canadian Geotechnical Journal*, vol. 52, no. 9, pp. 1199–1220, Feb. 2015, doi: 10.1139/CGJ-2014-0080.
- [9] K. R.-Civ. E. Publ. W. Rev. and undefined 1963, "The determination of strains in soils by an X-ray method," *ci.nii.ac.jp*, Accessed: Aug. 31, 2022. [Online]. Available: <https://ci.nii.ac.jp/naid/10012319105/>
- [10] R. James, "Stress and strain fields in sand," 1965, Accessed: Aug. 31, 2022. [Online]. Available: <https://www.repository.cam.ac.uk/handle/1810/283746>
- [11] D. J. White, M. D. Bolton, D. J. White, W. A. Take, and M. D. Bolton, "Measuring soil deformation in geotechnical models using digital images and PIV analysis SEE PROFILE Measuring soil deformation in geotechnical models using digital images and PIV analysis," pp. 997–1002, 2001, Accessed: Aug. 31, 2022. [Online]. Available: <https://www.researchgate.net/publication/237262677>
- [12] D. J. White, W. A. Take, and M. D. Bolton, "Soil deformation measurement using particle image velocimetry (PIV) and photogrammetry," *Geotechnique*, vol. 53, no. 7, pp. 619–631, 2003, doi: 10.1680/GEOT.2003.53.7.619.
- [13] D. White, W. Take, ... M. B.-P. of the, and undefined 2001, "A deformation measurement system for geotechnical testing based on digital imaging, close-range photogrammetry, and PIV image analysis," *researchgate.net*, 2001, Accessed: Aug. 31, 2022. [Online]. Available: [https://www.researchgate.net/profile/David-White-38/publication/303190522\\_A\\_deformation\\_measu](https://www.researchgate.net/profile/David-White-38/publication/303190522_A_deformation_measu)

- ring\_system\_for\_geotechnical\_testing\_based\_on\_digital\_imaging\_close\_range\_photogrammetry\_and\_PIV\_image\_analysis/links/5743188008aea45ee84b1940/A-deformation-measuring-system-for-geotechnical-testing-based-on-digital-imaging-close-range-photogrammetry-and-PIV-image-analysis.pdf
- [14] A. Rechenmacher, R. F.-G. T. Journal, and undefined 2004, "Digital image correlation to evaluate shear banding in dilative sands," *astm.org*, Accessed: Aug. 31, 2022. [Online]. Available: [https://www.astm.org/DIGITAL\\_LIBRARY/JOURNALALS/GEOTECH/PAGES/GTJ11263J.htm](https://www.astm.org/DIGITAL_LIBRARY/JOURNALALS/GEOTECH/PAGES/GTJ11263J.htm)
- [15] D. H. Beasley, "Centrifugal testing of models of embankments on soft clay foundations CambridgeUniversity PhD thesis," 1973.
- [16] R. Mair, "Centrifugal modelling of tunnel construction in soft clay," 1980, Accessed: Aug. 31, 2022. [Online]. Available: <https://www.repository.cam.ac.uk/handle/1810/283790>
- [17] H. Allersma, ... H. S.-I. conference, and undefined 1994, "Using image processing in soil mechanics," *pascal-francis.inist.fr*, Accessed: Aug. 31, 2022. [Online]. Available: <https://pascal-francis.inist.fr/vibad/index.php?action=getRecordDetail&idt=6347543>
- [18] R. Chaney, K. R. Demars, M. T. Obaidat, M. Taleb Obaidat, and M. F. Attom, "Computer vision-based technique to measure displacement in selected soil tests," *researchgate.net*, 1998, doi: 10.1520/GTJ10422J.
- [19] J. Chen, S. Robson, M. A. R. Cooper, and R. N. Taylor, "An evaluation of three different image capture methods for measurement and analysis of deformation within a geotechnical centrifuge," *International archives of photogrammetry and remote sensing*, vol. 31, no. B5, pp. 70–75, 1996.
- [20] R. Taylor, R. Grant, S. Robson, J. K.-C. 98, and undefined 1998, "An image analysis system for determining plane and 3-D displacements in soil models," *pascal-francis.inist.fr*, Accessed: Aug. 31, 2022. [Online]. Available: <https://pascal-francis.inist.fr/vibad/index.php?action=getRecordDetail&idt=6214398>
- [21] R. Grant, "Movements around a tunnel in two-layer ground," 1998, Accessed: Aug. 31, 2022. [Online]. Available: <https://openaccess.city.ac.uk/id/eprint/7569/>
- [22] R. A.-A. review of fluid mechanics and undefined 1991, "Particle-imaging techniques for experimental fluid mechanics," *academia.edu*, Accessed: Aug. 31, 2022. [Online]. Available: <https://www.academia.edu/download/73332358/fb3231b36d942b6ff1dacb8df68a6df9c9b0.pdf>